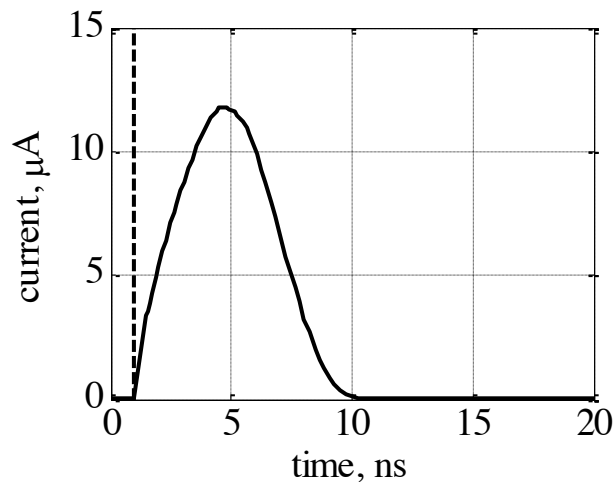

Progresses in LGAD simulations and comparison with experimental data from UFSD2, the new 50- μm production at FBK

Marco Mandurrino

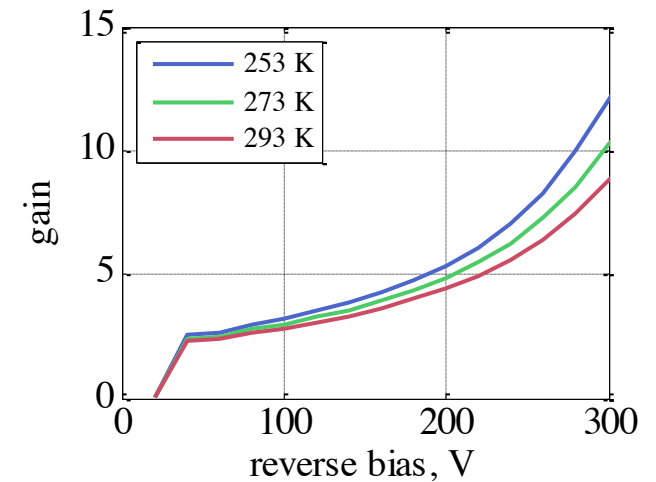
`marco.mandurrino@to.infn.it`

for the UFSD group (FBK, INFN Torino, Torino and Trento University)

1. Short recall about **Simulation Setup** and **Models Calibration**
 - **Gain** calculation procedure
 - Description of **avalanche models**
 - Empirical model for **acceptor removal**
 - **MIP calibration** in 50- μm thick *pin* diodes with laser/heavy-ion beam
2. The **UFSD2 production** by FBK
3. **Leakage current** and **Gain** simulations in UFSD2
 - **Boron/Gallium** implants
 - **Carbonated/non-carbonated** wafers
4. **Electric Field** and **Inter-pad Efficiency** simulations in UFSD2
 - Strip sensor **signal scan**



$$G(V) = \frac{Q_{LGAD}(V)}{Q_{pin}(V)}$$



The generation/recombination (GR) models accounted for in the simulation are:

- **Avalanche** generation
- **Shockley-Read-Hall (SRH)**
- **Band-to-band tunneling (BTBT)**

where three different multiplication models have been tested

van Overstraeten: $\alpha_{n,p}(E) = \gamma \cdot A_{n,p} \cdot \exp\left(-\gamma \frac{B_{n,p}}{E}\right)$

where: $A_n = 7.030 \times 10^5 \text{ cm}^{-1}$, $B_n = 1.231 \times 10^6 \text{ V/cm}$, $A'_p = 1.582 \times 10^6 \text{ cm}^{-1}$ and $B_p = 2.036 \times 10^6 \text{ V/cm}$ (or $A'_p = 6.710 \times 10^5 \text{ cm}^{-1}$ and $B'_p = 1.693 \times 10^6 \text{ V/cm}$ in low-field conditions)

Massey: $\alpha_{n,p}(E) = A_{n,p} \cdot \exp\left(-\frac{B_{n,p}(T)}{E}\right)$

where: $A_n = 4.43 \times 10^5 \text{ cm}^{-1}$, $A_p = 1.13 \times 10^6 \text{ cm}^{-1}$, $B_n(T) = C_n + D_n \cdot T$ and $B_p(T) = C_p + D_p \cdot T$, with $C_n = 9.66 \times 10^5 \text{ V} \cdot \text{cm}^{-1}$, $C_p = 1.71 \times 10^6 \text{ V} \cdot \text{cm}^{-1}$, $D_n = 4.99 \times 10^2 \text{ V} \cdot \text{cm}^{-1} \cdot \text{K}^{-1}$ and $D_p = 1.09 \times 10^3 \text{ V} \cdot \text{cm}^{-1} \cdot \text{K}^{-1}$

Okuto: $\alpha_{n,p}(E) = A_{n,p} \cdot (1 + (T - 300)C_{n,p}) \cdot E \cdot \exp\left(-\left(\frac{B_{n,p} \cdot (1 + (T - 300)D_{n,p})}{E}\right)^2\right)$

where: $A_n = 0.426 \text{ V}^{-1}$, $B_n = 4.81 \times 10^5 \text{ V/cm}$, $A_p = 0.243 \text{ V}^{-1}$, $B_p = 6.53 \times 10^5 \text{ V/cm}$, $C_n = 3.05 \times 10^{-4} \text{ K}^{-1}$, $C_p = 5.35 \times 10^{-4} \text{ K}^{-1}$, $D_n = 6.86 \times 10^{-4} \text{ K}^{-1}$ and $D_p = 5.67 \times 10^{-4} \text{ K}^{-1}$

Other transport models implemented in the drift-diffusion (DD) framework are the **Shockley-Read-Hall (SRH)** process, with generation rate

$$G_{\text{SRH}} = \frac{n \cdot p - n_i^2}{\tau_p (n - n_i \cdot \exp(-E_t/k_B T)) + \tau_n (p - n_i \cdot \exp(E_t/k_B T))}$$

and the **band-to-band tunneling (BTBT)**, where the rate is

$$G_{\text{BTBT}}(E) = A \cdot E^2 \cdot \exp\left(-\frac{B}{E}\right)$$

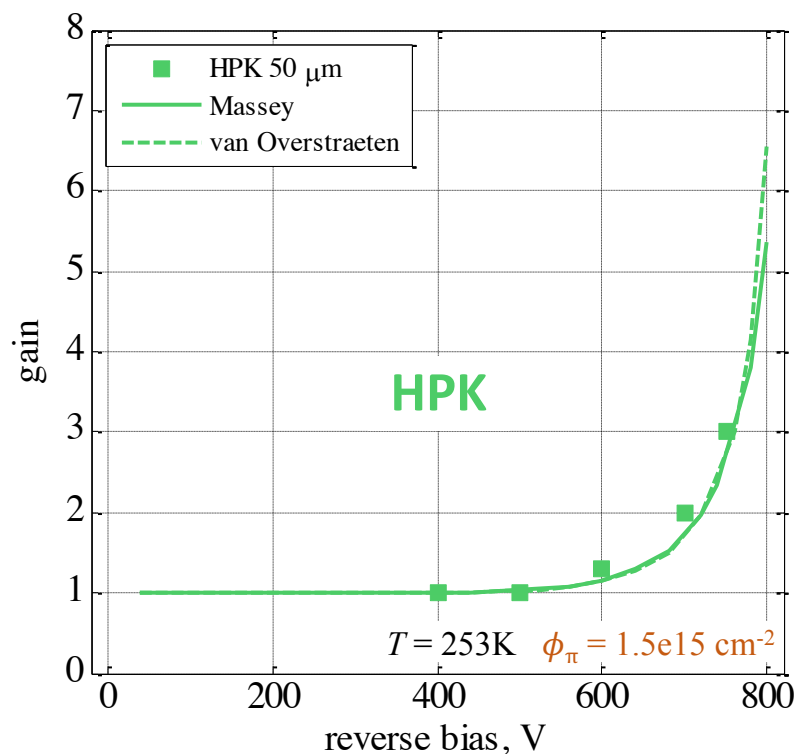
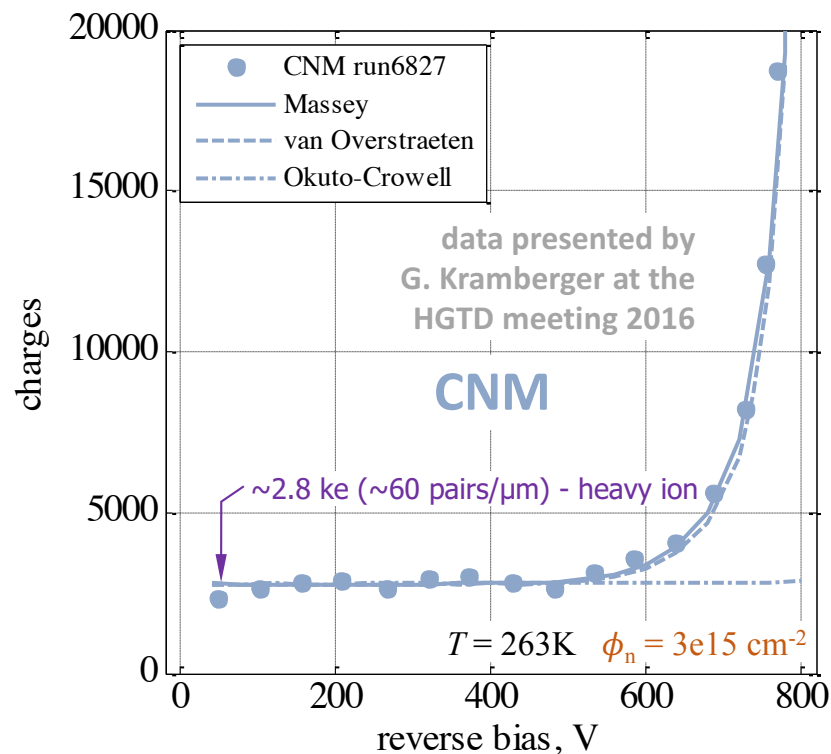
Concerning the **effects of radiation** we used the empirical law

$$N_A(\phi) = g_{\text{eff}} \cdot \phi + N_A(0) \cdot e^{-c(N_A(0)) \cdot \phi}$$

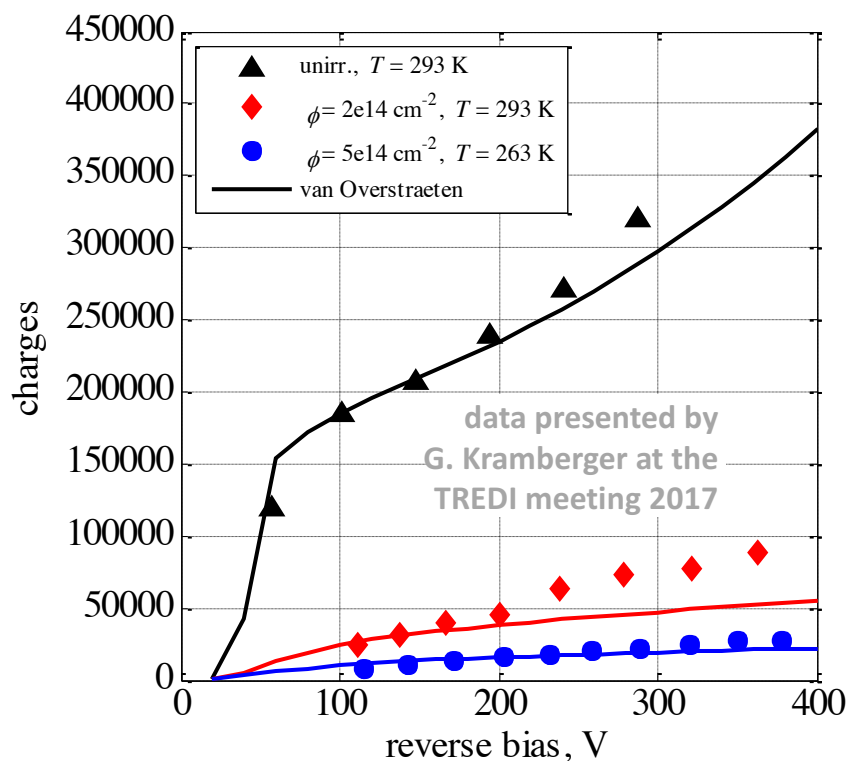
accounting for both **acceptor creation** and **initial acceptor removal** mechanisms, where ϕ is the fluence, $g_{\text{eff}} \cong 0.02 \text{ cm}^{-1}$ and

$$c(N_A(0), x) = \alpha \cdot N_A(0, x)^{-\beta}$$

MIP calibration on measurements from irradiated 50 μm *pin* diodes by CNM and HPK



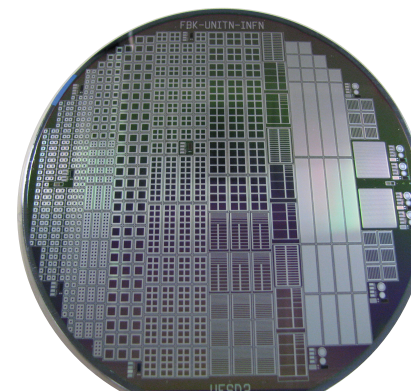
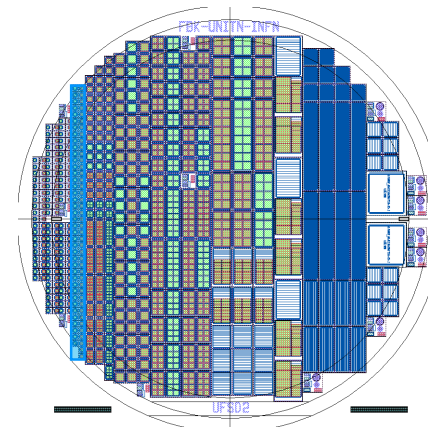
Example: irradiated **300 μm** UFSD by **FBK** at different **fluence** and **temperature**



- Simulation of both *pin* and **LGAD** diodes
- Measurements from **Ljubljana**
- Simulated heavy-ion at $\sim 60 \text{ pairs}/\mu\text{m}$
- **Acceptor removal** parametrization

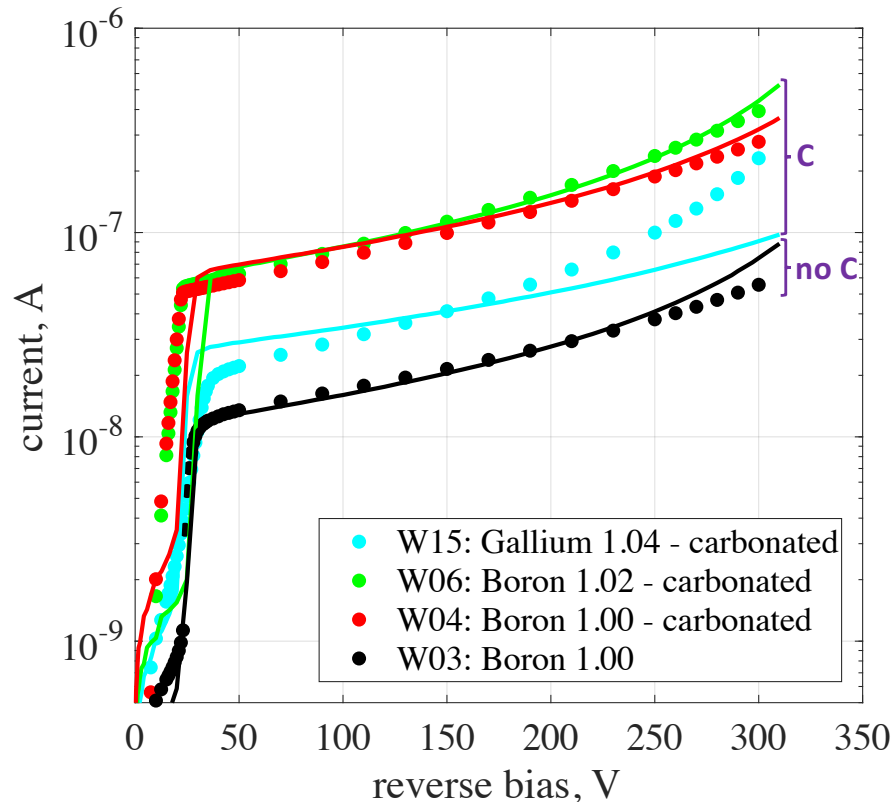
UFSD2 production

Wafer #	Dopant	Gain dose	Carbon
1	Boron	0.98	
2	Boron	1.00	
3	Boron	1.00	
4	Boron	1.00	low
5	Boron	1.00	High
6	Boron	1.02	low
7	Boron	1.02	High
8	Boron	1.02	
9	Boron	1.02	
10	Boron	1.04	
11	Gallium	1.00	
14	Gallium	1.04	
15	Gallium	1.04	low
16	Gallium	1.04	High
18	Gallium	1.08	



Non-irradiated 1 x 1 mm² pads

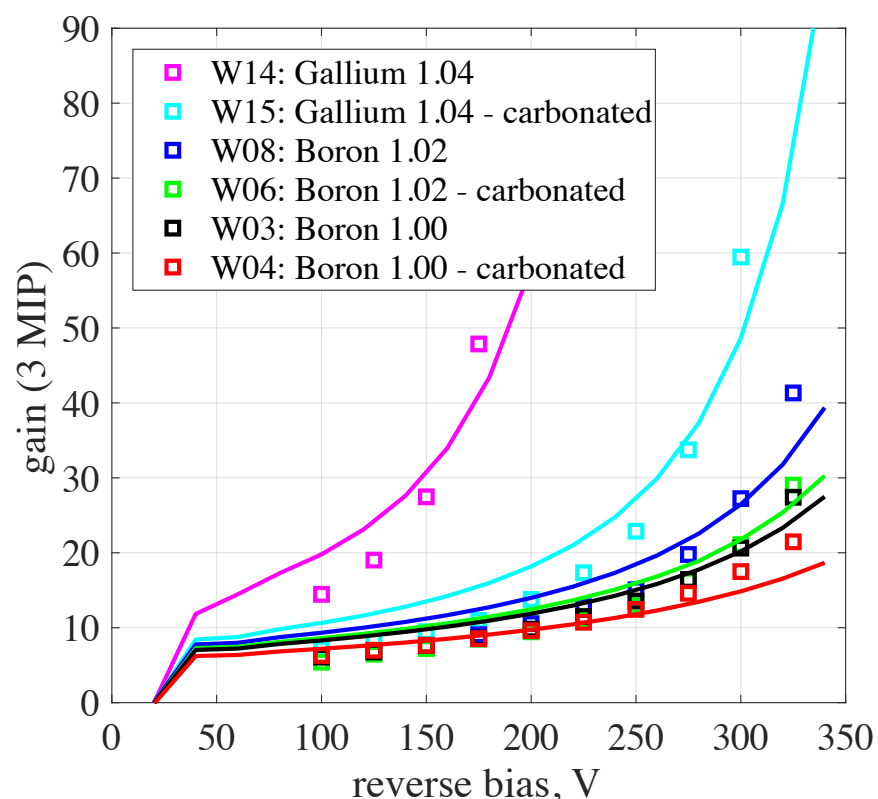
Leakage Current (on wafer)



- Simulations with **van Overstraeten - de Man** avalanche model and **focused laser beam**
 - Highly realistic **segmentation p and n profiles** (Montecarlo simulations)
 - **Gain layer implant profiles** coming from **$C(V)$ measurements**
- ⇒ **Non-carbonated devices show a lower leakage current**

Non-irradiated 1 x 1 mm² pads

Gain (laser setup)



- Simulations with **van Overstraeten - de Man** avalanche model and **focused laser beam**
- Highly realistic **segmentation p and n profiles** (Montecarlo simulations)
- **Gain layer** implant profiles coming from **$C(V)$ measurements**

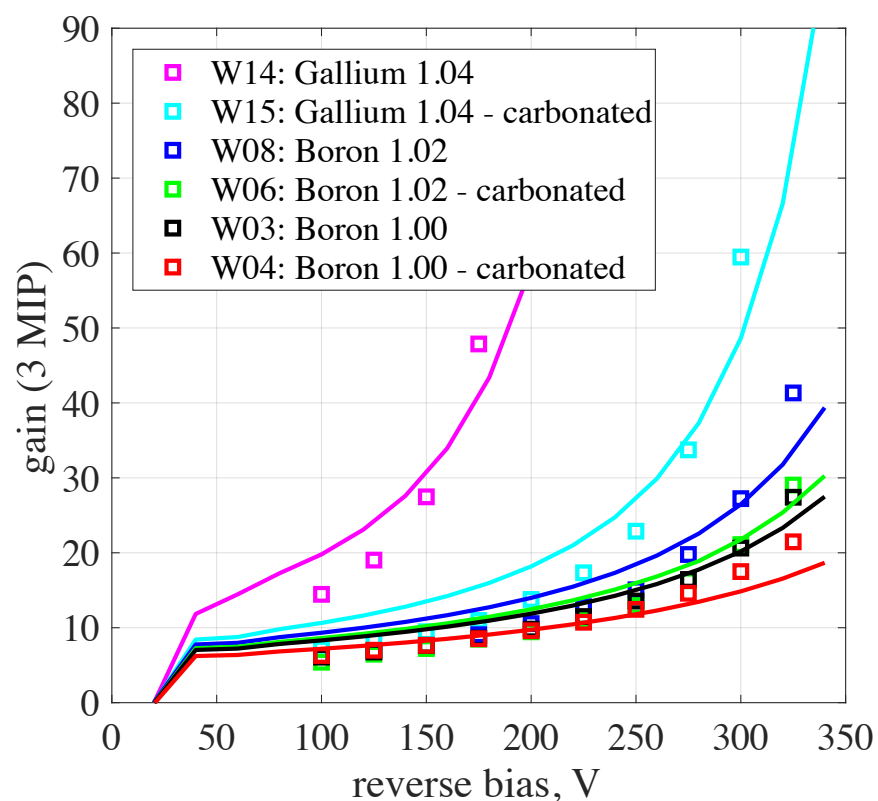
⇒ **Higher gallium/boron dose** corresponds to **higher gain**

⇒ **Carbon implantation** produces a **gain reduction**, especially in **Ga-doped wafers**

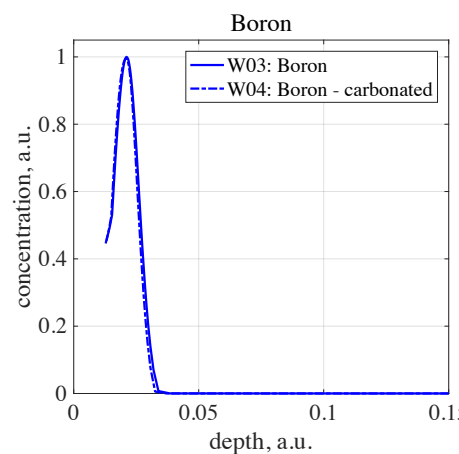
⇒ Possible **gallium/boron segregation** via **carbon clustering**

Non-irradiated 1 x 1 mm² pads

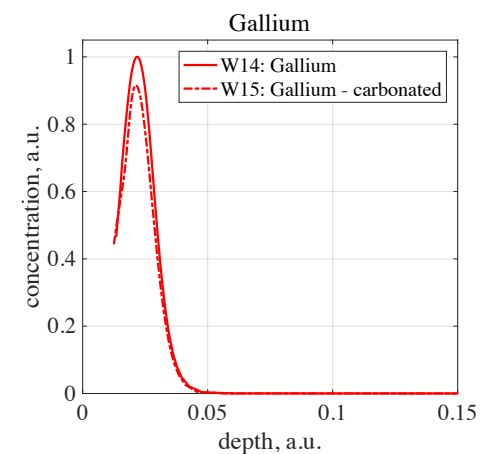
Gain (laser setup)



As stated by measured profiles...

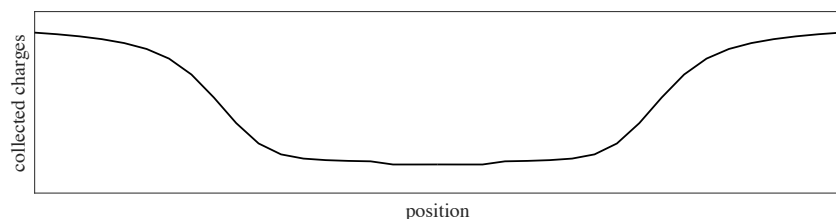
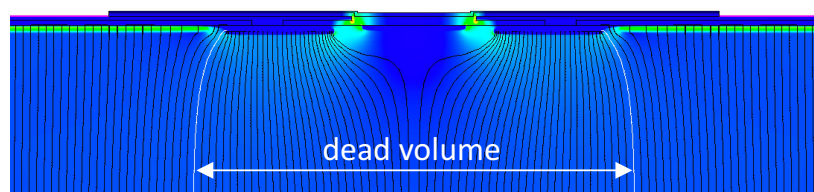
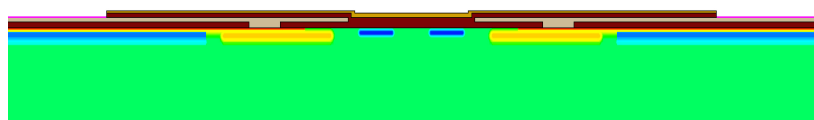


0.5% loss at peak



8.5% loss at peak

Non-irradiated ~200- μm pitch strips Electric Field



UFSD2 layout has been implemented

From Poisson equation

$$\nabla_{\mathbf{r}} E = \frac{\rho(\mathbf{r}, t)}{\epsilon}$$

one computes the **electric field**

Signal scan directly derives from the trend of **field lines** in the active region

The simulation setup used to **calibrate the TCAD framework** and to **investigate the UFSD1 production** was tested here on the new **UFSD2 sensors**

By implementing the **real gain profiles** it is possible to accurately reproduce the most important **static features of UFSD2**, like **leakage current** and **gain**

From the **electric field** calculation it is also possible to infer the **sensor efficiency** in the **inter-pad** region having, therefore, an estimation of the **fill-factor**

⇒ What's next?

- We are waiting data from the irradiation campaign on **UFSD-2 sensors** in order to test **multiplication** and **radiation-related** models on **Gallium-doped** and **carbonated** devices

Acknowledgments

This work was partly supported by the United States Department of Energy, **Grant DE-FG02-04ER41286**, and by the European Union's Horizon 2020 Research and Innovation funding program, under **Grant Agreement no. 654168** (AIDA-2020), **Grant Agreement no. 669529** (ERC UFSD669529), by the Italian **Ministero degli Affari Esteri (MAE)** and **INFN Gruppo V**.

Many thanks to: M. Boscardin, G. Paternoster, F. Ficorella (FBK)
L. Pancheri, G. F. Dalla Betta (Università di Trento)

Thank you for your attention!